A Hybrid Control Strategy for Robust Contact Detection and Force Regulation*

Raffaella Carloni‡, Ricardo G. Sanfelice†, Andrew R. Teel† and Claudio Melchiorri‡

***Abstract*— We present an innovative hybrid control strategy for contact detection and force regulation of robotic manipulators. This hybrid architecture controls the robotic manipulator during the following stages of interaction with the work environment: the free motion, the transition phase, and the constrained motion. The proposed control strategy is to switch between a position and a force controller with hysteresis relying only on contact force measurements. We implement this strategy in a hybrid controller and provide a design procedure which depends on the viscoelastic parameters of the work environment. Our controller guarantees contact detection and force regulation without bounce-off effects between the robotic manipulator and the work environment from compact sets of initial conditions. Additionally, the resulting closed-loop system is robust to measurement noise. We include simulations that show how the proposed hybrid control strategy guarantees good performance in the cases of stiff and compliant work environments, and in the presence of measurement noise.**

I. Introduction

Several complex robotic systems, such as grasping and locomotion devices, involve the interaction between a robotic manipulator and its work environment. The control issue of such type of tasks is the regulation of the transition phase, in which the dynamic of the system is switching from the free to the constrained motion. In particular, the crucial point of the control is in the detection of contact/non-contact states since, when the manipulator gets in contact with the environment, large impulsive forces can cause the manipulator to bounce off and to become unstable.

In the literature, the control of the dynamical behavior of the manipulator in interaction tasks has been a research topic for many years and several control synthesis schemes, both continuous and discontinuous, have been proposed. In the continuous case, the impedance control scheme is used to establish a desired dynamic relationship between the robotic manipulator position and the force it applies on the work environment [6], [7]. In the discontinuous case, the control scheme consists of a switching law in which a position controller is applied during non-contact motion while a position/force controller is applied during the transition phase and the contact stage [11], [8], [15], [10], [2]. Control algorithms that combine continuous and discontinuous features have been also proposed in the literature; in [13] an impedance control is used jointly with a hybrid system for the detection of the contact.

*Research partially supported by the Army Research Office under Grant no. DAAD19-03-1-0144, the National Science Foundation under Grant no. CCR-0311084 and Grant no. ECS-0622253, and by the Air Force Office of Scientific Research under Grant no. F9550-06-1-0134.

‡{rcarloni,cmelchiorri}@deis.unibo.it, Center for Research on Complex Automated Systems (CASY), Department of Electronics, Computer Science and Systems (DEIS), University of Bologna, Bologna 40136, Italy.

†{rsanfelice,teel}@ece.ucsb.edu, Center for Control Engineering and Computation, Electrical and Computer Engineering Department, University of California, Santa Barbara, CA 93106-9560.

In most cases, the contact/non-contact detection between the manipulator and the work environment is done on a surface which depends on position and velocity measurements. In the presence of measurement noise, such strategy can fail to detect the state of contact and, potentially, cause "chattering" in the controller. To avoid these issues, we propose a hybrid control strategy that switches between a position and a force controller with hysteresis. The position controller steers the manipulator to a target point in the workspace and the force controller regulates the force to a desired set-point. The detection of contact is accomplished with force information only. The proposed hybrid controller ensures regulation and stability of the force set-point and mitigates bouncing-off effects by limiting the impact velocity. Moreover, our control strategy confers a margin of robustness with respect to measurement noise in the position and force.

II. General Model

In this section, we present a dynamical model of a generic manipulator and a model of the reaction forces due to the interaction between the manipulator and the environment.

A. General Robotic Manipulator Model

The dynamic of the robotic manipulator in joint space is:

$$M(\theta)\ddot{\theta} + C(\theta,\dot{\theta})\dot{\theta} + N(\theta,\dot{\theta}) = \tau - J(\theta)^T f_c, \qquad (1)$$

where $M(\theta) \in \mathbb{R}^{n\times n}$ is the manipulator inertia matrix, $C(\theta,\dot{\theta}) \in \mathbb{R}^{n\times n}$ is the Coriolis matrix, $N(\theta,\dot{\theta}) \in \mathbb{R}^n$ includes gravity terms and other forces that act at the joints, $\tau \in \mathbb{R}^n$ is the vector of the actuators torques, $J(\theta) \in \mathbb{R}^{m\times n}$ is the Jacobian matrix relating the joint space velocity to the workspace velocity, and $f_c \in R^m$ is the vector of the contact forces due to the interaction between the manipulator and the environment. Since we are interested in the interactions, we rewrite the dynamic equation (1) in workspace coordinates x after a coordinate transformation from θ to x

$$\tilde{M}(\theta)\ddot{x} + \tilde{C}(\theta,\dot{\theta})\dot{x} + \tilde{N}(\theta,\dot{\theta}) = F - f_c,$$

where $\tilde{M},\tilde{C},\tilde{N}$ derive from M, C, N, and F is the vector of forces/torques applied at the end-effector of the manipulator.

B. Compliant Contact Force Model

Let $s : \mathbb{R}^m \to \mathbb{R}$ be a continuous function such that $S = \{x \in \mathbb{R}^m \mid s(x) = 0\}$ defines the surface of the environment without external interactions and $W = \{x \in \mathbb{R}^m \mid s(x) \leq 0\}$ defines the environment. Note that $s(x) \leq 0$ if x is a point in the environment and $s(x) > 0$ otherwise.

We consider the linear contact model of Kelvin-Voigt to characterize the relationship between the bodies' penetration and the reaction force [3]. In this model, the viscoelastic material of the environment is described as the mechanical

parallel of a linear spring and a damper which are represented, respectively, by a stiffness matrix $K_c \in \mathbb{R}^{m\times m}$ and a damper matrix $B_c \in \mathbb{R}^{m\times m}$. The contact force is given by

$$f_c = \begin{cases} K_c x + B_c \dot{x} & \text{if} \quad s(x) \leq 0 \\ 0 & \text{if} \quad s(x) > 0. \end{cases} \tag{2}$$

Figure 1 depicts this scenario and illustrates the compliant interaction between the robotic manipulator and the work environment. Due to the compliance there is compression of the bodies when the manipulator comes in contact with the environment. As in [8], [9], [10], [3], the compliance is modeled as part of the work environment, but our results are also applicable to scenarios with both compliance in the work environment and robotic manipulator.

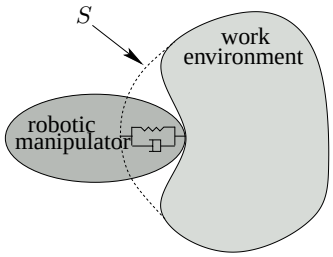

Fig. 1. The compliant contact force model is described by the mechanical parallel of a linear spring K_c and a damper B_c. S is the uncompressed work environment surface.

C. Model Reduction

With the knowledge of some of the parameters and state of the manipulator, it is possible to design an inner feedback loop that stabilizes some of the internal and external forces of the manipulator. Such technique is commonly used in robotic manipulator control literature, see e.g. [7], [15], [2]. Proceeding in this way, let u be the input control force in the workspace coordinates and let the inner feedback law

$$F = u + \tilde{C}(\theta, \dot{\theta})\dot{x} + \tilde{N}(\theta, \dot{\theta}) \ .$$

This feedback law is basically a state feedback linearization law that reduces the dynamics of the manipulator to

$$\tilde{M}(\theta)\ddot{x} = u - f_c. \tag{3}$$

As further described in [15], it is possible to distinguish between constrained and unconstrained direction of the motion of a manipulator interacting with an environment. Following [15], without loss of generality, we consider the case in which the interaction between the manipulator and its environment occurs along a normal direction. In this way, the manipulator consists simply of a mass with motion constrained to a straight line. The interaction with the work environment occurs at some point on that line. We further assume that the mass is unitary. Then, the dynamic of the manipulator gets reduced to the second-order system

$$\ddot{x} = u - f_c \tag{4}$$

where $x := [x_1 \ \ x_2] \in \mathbb{R}^2$, x_1 being the position and x_2 the velocity of the manipulator, and f_c is the contact force

$$f_c = \begin{cases} k_c x_1 + b_c x_2 & \text{if} \quad x_1 \geq 0 \\ 0 & \text{if} \quad x_1 < 0, \end{cases} \tag{5}$$

where $k_c, b_c \in (0, +\infty)$ are the elastic and the viscous parameters of the contact. Note that in the one-dimension case considered, the work environment gets reduced to $W = \{x_1 \in \mathbb{R} \mid x_1 \geq 0\}$ with surface $S = \{x_1 \in \mathbb{R} \mid x_1 = 0\}$.

III. Main Idea: Hysteresis Control based on Force Measurement

As discussed in the Introduction, the problem of contact detection and force regulation for robotic manipulators has previously been addressed in the literature. Perhaps the simplest strategy to accomplish the task described above is (whether contact/non-contact has been detected between the manipulator and the environment) to switch between a position controller, which steers the manipulator close to the environment, and a force controller, which regulates the force to a desired value. For example, when the position of the manipulator is $x_1 < 0$, the strategy is to use the position controller to steer the manipulator to a point in the interior of W and, when the position of the manipulator reaches S, the strategy is to use the force controller to regulate the contact force.

Figure 2 depicts a typical trajectory resulting from this switching logic. Note that several bounces and switches between the two controllers are present before the manipulator reaches the desired position/contact force configuration. Clearly, there exists a compact set of initial conditions for which there is no bounce-off effect (in Figure 2, such a compact set is a subset of a small enough neighborhood of the origin). However, in practice, this set is usually relatively small, as we will illustrate in Section VII. Moreover, with such control strategy, arbitrarily fast switching between the controllers can arise in the presence of measurement noise since, when the manipulator is in a neighborhood of the contact surface, even small measurement noise can indicate a false contact/non-contact condition.

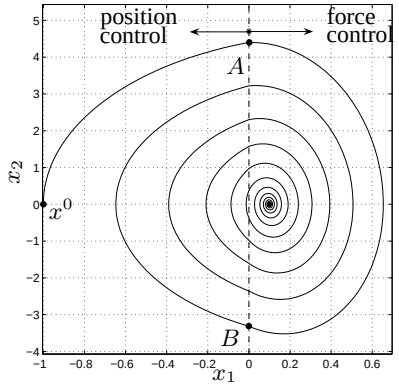

Fig. 2. Switching strategy based on position: the manipulator establishes and loses the contact in A and B, respectively. Several bounces (and switches between the position and force controllers) are present before the manipulator reaches the desired position and force configuration. x^0 is the initial condition.

We propose a control strategy that minimizes such issues. Let $0 < \gamma_1 < \gamma_2$,

1) with the manipulator starting away from the environment, apply a position controller until the contact force reaches a specified threshold γ_2;
2) with the manipulator in contact with the environment, maintain the force controller until the contact force is below a certain threshold γ_1.

This mechanism introduces hysteresis in the switches between the two controllers and, for this reason, it corresponds to a hybrid strategy.

The basic idea is illustrated in Figure 3. With the contact model (5), the contact force f_c is a linear combination of the two state variables x_1, x_2. Then, the conditions $f_c \geq \gamma_2$ and $f_c \leq \gamma_1$ for switching between the controllers correspond to half planes in the phase diagram. In particular these half planes have the lines $\ell_{\gamma_1} : \{(x_1, x_2) \mid x_2 = -\frac{k_c}{b_c} x_1 + \frac{\gamma_1}{b_c}\}$ and $\ell_{\gamma_2} : \{(x_1, x_2) \mid x_2 = -\frac{k_c}{b_c} x_1 + \frac{\gamma_2}{b_c}\}$ as their boundaries. (Note that these lines have fixed slope given by $-\frac{k_c}{b_c}$.) The sample trajectory in Figure 3 shows that the decision whether to apply the position controller is not on a single boundary line as in Figure 2, but on boundary lines $\ell_{\gamma_1}, \ell_{\gamma_2}$ that do not overlap. This separation between the switching lines makes the decision robust to small perturbations.

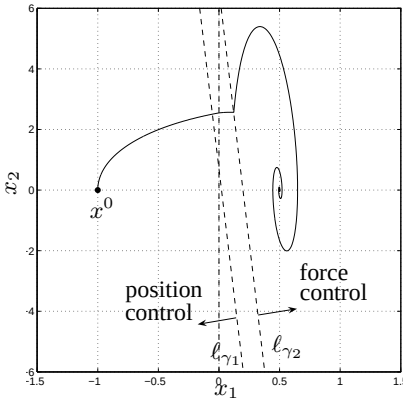

Fig. 3. Example of switching strategy based on hysteresis. ℓ_{γ_1} and ℓ_{γ_2} define the sets for the switches based on force. x^0 is the initial condition.

IV. Hybrid Controller for Robust Contact Detection

Now, we present the hybrid control strategy outlined in Section III. We follow the framework for hybrid systems in [4], [5] where solutions are given on *hybrid time domains* [1].

A. Position Controller

We consider a position controller for set-point stabilization of the position x_1 of the manipulator in (4) that relies on position and velocity measurements of the manipulator and is given by the proportional/derivative control law

$$\kappa_P(x, x_1^d) = -k_p(x_1 - x_1^d) - k_d x_2 \tag{6}$$

where $x_1^d > 0$ is the position set-point and $k_p, k_d \in \mathbb{R}$ are constants to be designed. Proportional/derivative controllers have been previously used in the literature for set-point stabilization of manipulators, e.g. [7], [8], [15].

B. Force Controller

Let f_c^d, $0 < f_c^d < \hat{f}_c$, be the desired set-point for the contact force where $\hat{f}_c$ is the maximum allowed force. We consider a force controller that only relies on measurements of the contact force and that is given by the proportional/feedforward control law

$$\kappa_F(f_c, f_c^d) = f_c + k_f(f_c^d - f_c) \tag{7}$$

where $k_f \in \mathbb{R}$ is a constant to be designed. Similar force control strategies have been considered in [8], [9].

[1] In this framework, a solution x to a hybrid system on a hybrid time domain $\mathrm{dom}\, x$ is parameterized by a continuous variable t which keeps track of the continuous dynamics and a discrete variable j which keeps track of the discrete dynamics. Then, $x(t, j)$ is the value of the solution at time $(t, j) \in \mathrm{dom}\, x$. For more details, see [4], [5].

C. Control Strategy

The main idea of the control strategy for contact detection outlined in Section III is to switch from position to force controller (and vice versa) relying only on information of measurements of the contact force. We consider the simple controllers in IV-A, IV-B, but the strategy is applicable to more sophisticated controllers. The key feature of this strategy is that the controller selection depends on the memory of the controller; hence, it is a (logic-based) hybrid controller.

We implement the control strategy in a hybrid controller which we denote by $\mathcal{H}_c$. The state of the controller is given by the logic variable $q \in Q := \{0, 1\}$. Let the constants threshold levels $\gamma_1, \gamma_2 \in \mathbb{R}_{>0}$ be parameters of $\mathcal{H}_c$.

As depicted in Figure 4, the update law for the logic variable q is so that it switches between 0 and 1 based on the value of f_c with hysteresis levels defined by γ_1, γ_2. Two different transitions are possible:

- $q = 0 \to 1$ (path: $0 \to A \to B \to C$): The logic variable q can only be mapped to 1 when the measured contact force reaches the threshold γ_2 (when $f_c \geq \gamma_2$).
- $q = 1 \to 0$ (path: $C \to B \to D \to 0$): The logic variable q can only be mapped to 0 when the measured contact force is below the threshold γ_1 (when $f_c \leq \gamma_1$).

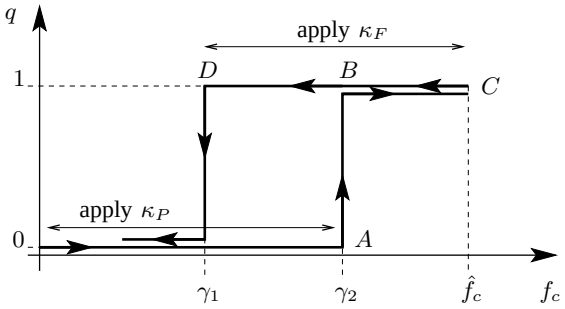

Fig. 4. Contact detection strategy with hysteresis. Constants γ_1, γ_2 define the thresholds for change from mode $q = 0$ to mode $q = 1$ (and vice versa).

The dynamics of the hybrid controller $\mathcal{H}_c$ are as follows.

Jumps:

- From $q = 0$ to $q = 1$ (i.e. $q^+ = 1$): when $q = 0$ and $f_c \geq \gamma_2$, the logic variable q is mapped to 1.
- From $q = 1$ to $q = 0$ (i.e. $q^+ = 0$): when $q = 1$ and $f_c \leq \gamma_1$, the logic variable q is mapped to 0.

Flows:

- $\dot{q} = 0$: when $q = 0$ and $f_c \leq \gamma_2$, or when $q = 1$ and $f_c \geq \gamma_1$, the logic variable remains constant.

The output of the controller is given by

$$u := \kappa(x, f_c, x_1^d, f_c^d, q) := \begin{cases} \kappa_P(x, x_1^d) & \text{if} \quad q = 0 \\ \kappa_F(f_c, f_c^d) & \text{if} \quad q = 1 \end{cases}.$$

Remark 4.1: The logic variable q indicates whether it is "safe" or not to switch from the position controller κ_P to the force controller κ_F. The switches between position/force controllers occur when bounces off the work environment are not possible: when a certain level of contact force has been achieved, switching from the position controller to the force controller is enabled. Note that the hybrid controller $\mathcal{H}_c$ switches from κ_P to κ_F if the logic variable q makes a transition $0 \to 1$. This is possible only if the position controller is able to generate a contact force that is larger than γ_2 and if the measurement of f_c experiences an increase

of at least $\gamma_2 - \gamma_1 > 0$. Vice versa, the hybrid controller $\mathcal{H}_c$ switches from κ_F to κ_P if the logic variable q makes a transition $1 \to 0$. This is possible only if the measurement of f_c experiences a decrease of at least $\gamma_2 - \gamma_1 > 0$. ■

D. Closed-loop System

The closed-loop system, denoted by $\mathcal{H}_{cl}$ and depicted in Figure 5, resulting of controlling (4) with the hybrid controller $\mathcal{H}_c$, has continuous dynamics given by

$$\left.\begin{array}{ll} \dot{x}_1 & = x_2 \\ \dot{x}_2 & = \kappa(x, f_c, x_1^d, f_c^d, q) - f_c \\ \dot{q} & = 0 \end{array}\right\} \ (x,q) \in C$$

where $C := C_0 \cup C_1 \subset \mathbb{R}^2 \times Q$ defines the flow set, where:

$$\begin{array}{rcl} C_0 & := & \{(x,q) \in \mathbb{R}^2 \times Q \mid q = 0 \ \text{ and } \ f_c \leq \gamma_2\} \\ C_1 & := & \{(x,q) \in \mathbb{R}^2 \times Q \mid q = 1 \ \text{ and } \ f_c \geq \gamma_1\}. \end{array}$$

The closed-loop system $\mathcal{H}_{cl}$ has jump dynamics given by

$$\begin{array}{l} x_1^+ = x_1, \quad x_2^+ = x_2, \quad q^+ = 1, \quad (x,q) \in D_0 \\ x_1^+ = x_1, \quad x_2^+ = x_2, \quad q^+ = 0, \quad (x,q) \in D_1 \end{array}$$

$$\begin{array}{l} D_0 := \{(x,q) \in \mathbb{R}^2 \times Q \mid q = 0 \ \text{ and } \ f_c \geq \gamma_2\} \\ D_1 := \{(x,q) \in \mathbb{R}^2 \times Q \mid q = 1 \ \text{ and } \ f_c \leq \gamma_1\} \end{array}$$

and the jump set is $D := D_0 \cup D_1 \subset \mathbb{R}^2 \times Q$.

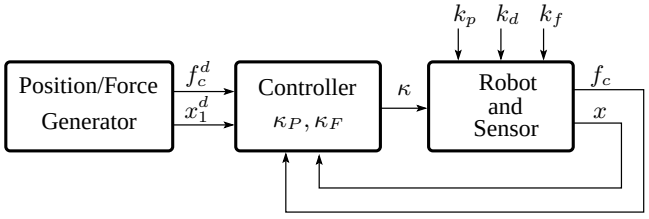

Fig. 5. Hybrid control scheme. A position/force block generates the set-points f_c^d and x_1^d. The controller has as input the position of the manipulator x in the workspace coordinates and the measured contact force f_c.

V. Controller Design

We now design the hybrid controller, for given parameters k_c, b_c of the work environment and desired contact force f_c^d. The parameters to design for are k_f, k_p, k_d, γ_1, γ_2 and x_1^d. We state the following results that are used in the design.

Lemma 5.1: For every given parameters $k_c, b_c \in (0, +\infty)$ of the work environment and desired contact force $0 < f_c^d < \hat{f}_c$, there exist $k_f \in \mathbb{R}$, $P_f, Q_f \in \mathbb{R}^{2\times 2}$, $P_f = P_f^T > 0$, $Q_f = Q_f^T > 0$, such that

$$\langle \nabla V_F(z), f(z) \rangle = -z^T Q_f z \quad \forall z \in \mathbb{R}^2, \tag{8}$$

$$[1/k_c \quad -1/b_c]^T \in eigv\{P_f\}, \tag{9}$$

where $V_F(z) = z^T P_f z$ and

$$f(z) := \left[-k_f k_c \left(z_1 + \frac{f_c^d}{k_c} \right)^{z_2} - k_f b_c z_2 + k_f f_c^d \right].$$

Furthermore, P_f, Q_f, and k_f are given by

$$P_f := \begin{bmatrix} a & c \\ c & b \end{bmatrix} = R \begin{bmatrix} p_1 & 0 \\ 0 & p_2 \end{bmatrix} R^T, \tag{10}$$

$$Q_f = \begin{bmatrix} 2ck_ck_f & (bk_c + cb_c)k_f - a \\ (bk_c + cb_c)k_f - a & 2(bb_ck_f - c) \end{bmatrix}, \tag{11}$$

$$k_f \in \left(0, \frac{-2c^2k_c + abk_c + acb_c}{(bk_c - cb_c)^2}\right), \tag{12}$$

with $R := \begin{bmatrix} -\sin\beta & -\cos\beta \\ \cos\beta & -\sin\beta \end{bmatrix}$ *and* $p_1, p_2 > 0$ *satisfying*

$$p_2 < p_1, \quad \frac{p_1 \sin^2\beta + p_2 \cos^2}{(p_2 - p_1)\sin\beta\cos\beta} < 2\frac{k_c}{b_c}. \tag{13}$$

Let $x_1^F := \frac{f_c^d}{k_c}$. Lemma 5.1 states that, given parameters k_c, b_c of the work environment and a desired contact force $0 < f_c^d < \hat{f}_c$, there exists a positive definite matrix P_f such that $V_F(x) := a(x_1 - x_1^F)^2 + bx_2^2 + 2c(x_1 - x_1^F)x_2$ is a Lyapunov function for the system (4) controlled by κ_F. We use this Lyapunov function to design the hysteresis thresholds γ_1 and γ_2. Note that P_f is the clockwise rotation of a positive definite diagonal matrix.

Figure 6 depicts these two lines and a level set of V_F. These lines are parallel and are parameterized by γ_1 and γ_2, respectively. The design of γ_1, γ_2 and x_1^d is as follows.

a) γ_1 min value: $\gamma_{1_{\min}} = 0$.

b) γ_1 max value: $\gamma_{1_{\max}} = x_1^F \left(k_c - \sqrt{\frac{k_c^2 b - 2ck_cb_c + ab_c^2}{b}} \right)$

c) x_1^d min value: $x_{1_{\min}}^d = x_1^F b_c \frac{c}{b} \frac{k_p + k_c}{k_p k_c}$

d) γ_2 min value: $\gamma_{2_{\min}} = b_c \frac{c}{b} x_1^F$

e) γ_2 max value: $\gamma_{2_{\max}} = k_c \min\{\frac{k_p}{k_p + k_c} x_{1_{\min}}^d, x_1^F\}$

Then, by considering $\gamma_1 \in [\gamma_{1_{\min}}, \gamma_{1_{\max}}]$, $\gamma_2 \in [\gamma_{2_{\min}}, \gamma_{2_{\max}}]$, $x_1^d \in [x_{1_{\min}}^d, +\infty)$, k_f given by Lemma 5.1 and with $k_p, k_d > 0$, the design of $\mathcal{H}_c$ is completed.

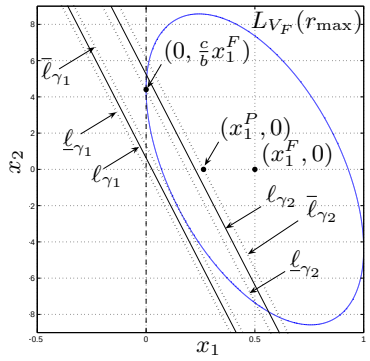

Fig. 6. Design of the hybrid controller $\mathcal{H}_c$. Lines $\underline{\ell}_{\gamma_1}$, $\overline{\ell}_{\gamma_1}$, $\underline{\ell}_{\gamma_2}$, $\overline{\ell}_{\gamma_2}$ are the upper/lower bound for the design of ℓ_{γ_1} and ℓ_{γ_2}, respectively. $x_1^P = \frac{k_p}{k_p + k_c} x_1^d$. $(x_1^P, 0)$, $(x_1^F, 0)$ are the equilibrium points of the system with the position and force controller, respectively. $L_{V_F}(r_{\max})$ is the maximum level set of V_F such that $\{x \in \mathbb{R}^2 : V_F(x) \leq r_{\max}\} \subset \mathbb{R}_{\geq 0}$.

Remark 5.2: The threshold γ_2 is designed so to guarantee that the manipulator does not bounce off the surface of the environment and so that the trajectory of the system remains all contained in the right half plane, after the hit with the environment. This means that the switch has to occur once the trajectory of the system is already inside the basin of attraction $L_{V_F}(r_{\max})$[1] of the system controlled in force. In order to grant that, at least, there is one switch between the position and the force controllers, the trajectory has to hit the threshold line ℓ_{γ_2} before reaching the equilibrium point

[1] $L_{V_F(r_{\max})}$ is the maximum level set of the Lyapunov function V_F such that $\{x \in \mathbb{R}^2 : V_F(x) \leq r_{\max}\} \subset \mathbb{R}_{\geq 0}$.

$(x_1^P, 0)$, $x_1^P := \frac{k_p}{k_p+k_c} x_1^d$. Moreover, the line ℓ_{γ_2} has also to be on the right of the equilibrium point $(x_1^F, 0)$.

For the design of the threshold γ_1, the lower bound for ℓ_{γ_1} is given by zero. Moreover, we design the line ℓ_{γ_1} so that it does not intersect the level set $L_{V_F}(r_{\max})$. The second condition in (13) implies that $\gamma_{1_{\min}} < \gamma_{1_{\max}}$. The parameters $k_p, k_d > 0$ are not constrained in principle, but they determine the size of the region of attraction of $\mathcal{H}_{cl}$. ■

VI. Main Results

The main stability and robustness properties of the closed-loop system $\mathcal{H}_{cl}$ are stated below. The following two results guarantee that the position controller κ_P steers the trajectories to a point in the interior of the work environment.

Lemma 6.1: For every given parameters $k_c, b_c \in (0, +\infty)$ of the work environment, controller parameters k_p, k_d, x_1^d, γ_1, γ_2 given from the design in Section V, the equilibrium point $(x_1^d, 0)$ to

$$\dot{x}_1 = x_2, \quad \dot{x}_2 = -k_p\ x_1 - k_d\ x_2 + k_p\ x_1^d \tag{14}$$

is globally asymptotically stable. Moreover, every solution to (14) starting from $x^0 \in \mathbb{R}^2$ reaches the set $S_1 := \{x \in \mathbb{R}^2 \mid x_1 \geq 0\}$ in finite time. In particular, for every initial condition $x^0 \in S_1^c := (\mathbb{R}^2 \setminus S_1) \cap \{x \in \mathbb{R}^2 \mid x_2 \geq 0\}$, every solution is such that $x_2(T) > 0$, where $T > 0$, is the time to reach S_1.

Lemma 6.2: For every given parameters $k_c, b_c \in (0, +\infty)$ of the work environment, controller parameters k_p, k_d, x_1^d, γ_1, γ_2 given from the design in Section V, the equilibrium point $\left(\frac{k_p}{k_p+k_c} x_1^d, 0\right)$ to

$$\dot{x}_1 = x_2, \quad \dot{x}_2 = -(k_p + k_c)\ x_1 - (k_d + b_c)\ x_2 + k_p\ x_1^d \tag{15}$$

is globally asymptotically stable. Moreover, every solution to (15) starting from $x^0 \in \mathbb{R}^2$ reaches the set $S_2 := \{x \in \mathbb{R}^2 \mid k_c x_1 + b_c x_2 \geq \gamma_2, x_1 \geq 0\}$ in finite time. In particular, for every initial condition $x^0 \in S_2^c := (\mathbb{R}^2 \setminus S_2) \cap \{x \in \mathbb{R}^2 \mid x_2 \geq 0\}$, every solution is such that $x_2(T) \geq 0$, where $T \geq 0$, is the time to reach S_2.

The proof of Lemmas 6.1 and 6.2 follow by simple Lyapunov and invariance arguments. In particular, it is easy to find quadratic Lyapunov functions that show global asymptotic stability of the origin in both lemmas. Combining these Lyapunov functions, the set of initial conditions for contact detection and contact force regulation can be computed. The following result establishes that those sets are "subsets" of the basin of attraction of the closed-loop system. Let $\mathcal{A} := \{(x_1^F, 0)\}$.

Theorem 6.3: Given parameters $k_c, b_c \in (0, +\infty)$ of the work environment and desired contact force $0 < f_c^d < \hat{f}_c$, there exist

1) *Compact sets $K_0, K_1 \subset \mathbb{R}^2$,*
2) *Parameters $k_f, k_p, k_d, \gamma_1, \gamma_2, x_1^d$ of the hybrid controller such that $\mathcal{A} \times \{1\}$ is locally asymptotically stable with basin of attraction containing $(K_0 \times \{0\}) \cup (K_1 \times \{1\}) \cap (C \cup D)$.*

The set of initial conditions K_0 is such that, for every initial condition $x^0 \in K_0$ of the manipulator and for given parameters of the position controller, the manipulator reaches the surface of the work environment with a bounded value of the impact velocity, denoted by x_2^*. As mentioned above, it can be explicitly computed combining the Lyapunov functions in Lemma 6.1 and Lemma 6.2. The set of initial conditions K_1 can be estimated with the maximum level set of V_F that is contained in $x_1 \geq 0$, that is, $L_{V_F}(r_{\max})$.

In the presence of measurement noise in both position and force, the asymptotic stability property above is preserved in a practical sense.

Theorem 6.4: There exists $\beta \in \mathcal{KL}$, for each $\varepsilon > 0$ and each compact set $K_0, K_1 \subset \mathbb{R}^2$ such that $(K_0 \times \{0\}) \cup (K_1 \times \{1\})$ is a subset of the basin of attraction of $\mathcal{H}_{cl}$, there exists $\delta^* > 0$, such that for each position and force measurement noise $e : \mathbb{R}_{\geq 0} \to \delta^* \mathbb{B}$, solutions (x, q) to $\mathcal{H}_{cl}$ exist, are complete, and for initial conditions $(x^0, q^0) \in (K_0 \times \{0\}) \cup (K_1 \times \{1\})$ the x component of the solutions satisfies [2]

$$|x(t,j)|_{\mathcal{A}} \leq \beta(|x^0|_{\mathcal{A}}, t + j) + \varepsilon \quad \forall (t,j) \in \mathrm{dom}(x, q)\ .$$

Note that the constraint on impact velocity in our control algorithm implies that the compact set of initial conditions guaranteed to exist by Theorem 6.4 is no larger than the one in Theorem 6.3. The proof of Theorem 6.4 follows by the properties of the closed-loop system $\mathcal{H}_{cl}$ and the results for perturbed hybrid systems in [5]. Due to space limitations, we do not discuss the concept/issues on existence of solutions with measurement noise; see [12] for more details.

VII. Simulations

In this section, we provide simulation results of the closed-loop system in the nominal case and in the presence of noise in the measurements of f_c. We illustrate the design of the hybrid controller for a set of parameters k_c, b_c, f_c^d, and present simulations for different materials of the environment.

Nominal case. Let the work environment be given by $W = \{x_1 \in \mathbb{R} \mid x_1 \geq 0\}$ and be characterized by a soft material with stiffness $k_c = 10$ N/mm and damping coefficient $b_c = 0.3$ Ns/mm. Let the desired force be $f_c^d = 5$ N. From these parameters, we compute $\beta = \arctan(-k_c/b_c)$ and $x_1^F = f_c^d/k_c = 0.5$ mm. By Lemma 5.1, we construct $P_f = [a\ c; c\ b]$ where $a = 2$, $b = 0.01$ and $c = 0.06$ satisfying (10) and we choose $k_f = 40$ which satisfies (12). Performing the computations in a)-e) in Section V we obtain: $\gamma_{1_{\min}} = 0$ N, $\gamma_{1_{\max}} = 0.71$ N, $x_{1_{\min}}^d = 0.79$ mm, $\gamma_{2_{\min}} = 1.32$ N, $\gamma_{2_{\max}} = 2.64$ N. Then, we pick $\gamma_1 = 0.61$ N, $\gamma_2 = 1.98$ N and $x_1^d = 1.58$ mm which satisfy the respective bounds. To complete the design, we follow Lemmas 6.1 and 6.2 and choose $k_p = 2$ and $k_d = 0.5$. Figure 7 illustrates a closed-loop trajectory. The position control steers the manipulator to the work environment until the measured contact force is equal to the threshold line denoted ℓ_{γ_2}. At this point, the hybrid controller switches to the force controller and the contact force is regulated to f_c^d. To accomplish this force level, the state of the manipulator is regulated to $(x_1^d, 0)$. Notice that no bounces off the work environment occur. This is accomplished by the controller logic which is such that, as long as the impact velocity is no larger than $x_2^* = 4.4$ mm/s, switches to the force controller are enabled only when the manipulator state is in $L_{V_F}(r_{\max})$ with $r_{\max} = 0.18$, contained in the right-half plane.

In Figure 8, we show closed-loop trajectories resulting from controllers designed for soft, stiff, and very stiff materials; i.e. for k_c increasing. As summarized in Table I, note

[2] Given a set $U \subset \mathbb{R}^n$ and a point $x \in \mathbb{R}^n$, $|x|_U = \inf_{y \in U} |x - y|$. Recall that $\mathrm{dom}(x, q)$ denotes the domain of the solution (x, q).

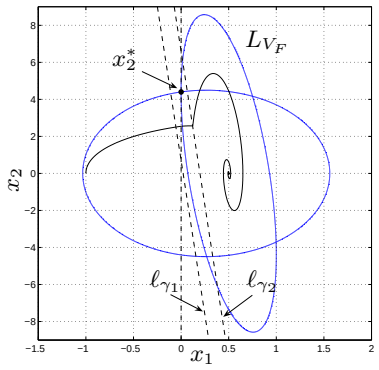

Fig. 7. Phase diagram of the switching strategy. The plot depicts the Lyapunov functions level sets of position/force controller, the ℓ_{γ_1} and ℓ_{γ_2} lines, and the trajectory of the system. The initial condition is $x_1^0 = -1$ mm, $x_2^0 = 0$ mm/s, and $q^0 = 0$. Maximum impact velocity is $x_2^* = 4.4$ mm/s.

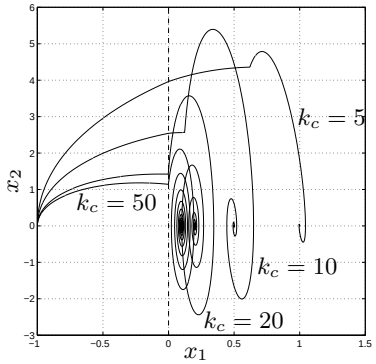

Fig. 8. Phase diagram of the switching strategy: different trajectories of the system for values of the environment material stiffness equal to $5, 10, 25, 50$ N/mm. The steady state point is changing since $x_1^F = f_c^d/k_c$.

that to avoid bounces, as the stiffness of the environment is increasing, the maximum allowed impact velocity decreases. The parameter x_1^d also decreases in order to satisfy the set-point $f_c^d = 5$N. This shows that our algorithm guarantees performance by constraining the maximum velocity of impact. Moreover, for fixed k_c, b_c, there is a trade-off between the maximum admitted impact velocity and the gain k_f of the force controller: in particular, in order to have a large impact velocity, a large gain is required. In addition, the data in the last two columns are an indicator of the improvement of our hybrid control strategy upon the discontinuous control law in Section III. By simulation, we compute the value of $x_1^0 < 0$ (given in millimeters) farthest away from the work environment such that solutions to $\mathcal{H}_{cl}$ from $(x_1^0, 0)$, x_1^0 given by column ($\mathcal{H}_{cl}$), and solutions to the closed-loop system with the discontinuous law from $(x_1^0, 0)$, x_1^0 given by column (disc.), do not bounce off. The controllers and parameters used for the simulations are fixed for each row.

Measurement noise case. Figure 9 depicts in dashed line the trajectory of the system without noise, and in continuous the trajectories of the system with different values of noise in the measurement of f_c: we have added a Gaussian noise with zero mean and variation of $\sigma = 0.01, 0.5, 1, 2$. Note that the hybrid controller is still able to steer trajectories to x_1^F without bounces.

TABLE I

CONTROLLER DESIGN PARAMETERS FOR VARIABLE k_c, FIXED b_c.

k_c(N/mm)	x_1^d(mm)	x_2^*(mm/s)	k_f	$(\mathcal{H}_{cl})$	$(disc.)$
1	14.5581	16.1757	430	-4.526	-0.6
5	4.1208	9.8115	80	-4.13	-0.1
10	1.5843	4.4007	16	-2.44	-0.08
20	0.4530	1.3727	20	-0.83	-0.06
50	0.0736	0.2360	8	-0.32	-0.055
100	0.0182	0.0596	4	-0.11	-0.051
200	0.0045	0.0149	2	-0.05	-0.03
500	0.0007	0.0024	0.8	-0.03	-0.02

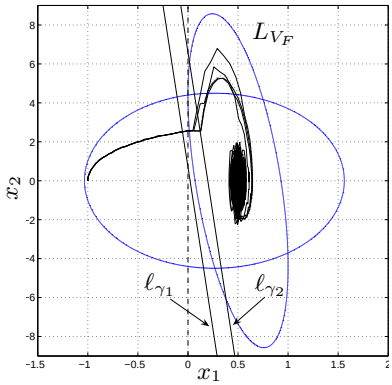

Fig. 9. Phase diagram of the switching strategy in presence of noise in the measurement of f_c. The plot depicts the Lyapunov functions level sets of the position/force controllers, the ℓ_{γ_1} and ℓ_{γ_2} lines, the trajectory of the system both without noise (dashed) and different values of noise (continuous).

REFERENCES

[1] B. Brogliato, P. Orhant, "Contact Stability Analysis of a One Degree-of-Freedom Robot", *Dynamics and Control*, vol. 8, pp 37-53, 1998.

[2] M. C. Çavuşoğlu, J. Yan, S. S. Sastry, "A Hybrid System Approach to Contact Stability and Force Control in Robotic Manipulators", *Proc. 12th IEEE Intern. Symp. on Intelligent Control*, pp 143-148, 1997.

[3] G. Gilardi, I. Sharf, "Literature Survey of Contact Dynamics Modelling", *Mechanism and Machine Theory*, vol. 18, pp 1213-1239, 2002.

[4] R. Goebel, J. P. Hespanha, A. R. Teel, C. Cai, R. G. Sanfelice, "Hybrid Systems: Generalized Solutions and Robust Stability", *Proc. 6th IFAC Symposium in Nonlinear Control Systems*, pp 1-12, 2004.

[5] R. Goebel, A. R. Teel, "Solutions to Hybrid Inclusions Via Set and Graphical Convergence with Stability Theory Applications", *Automatica*, vol. 42, n. 4, pp 573-587, 2006.

[6] N. Hogan, "Impedance Control: An approach to Manipulation: Part I Theory", *ASME Jour. of Dynamic Systems, Measurement and Control*, vol. 107, pp 335-345, 1985.

[7] O. Khatib, "A Unified Approach for Motion and Force Control of Robot Manipulators: The Operational Space Formulation", *IEEE Trans. on Robotics and Automation*, vol. RA-3, n. 1, pp 43-53, 1987.

[8] J. K. Mills, D. M. Lokhorst, "Stability and Control of Robotic Manipulators During Contact/Noncontact Task Transition", *IEEE Transaction on Robotics and Automation*, vol. 9, n. 3, pp 335-345, 1993.

[9] R. M. Murray, Z. Li, S. S. Sastry, *A Mathematical Introduction to Robotic Manipulation*, CRC Press, Boca Raton, 1994.

[10] P. R. Pagilla, M. Tomizuka, "Contact Transition Control of Nonlinear Mechanical Systems Subject to a Unilateral Constraint", *ASME Jour. of Dyn. Sys., Measurement and Control*, vol. 119, pp 749-759, 1997.

[11] M. H. Raibert, J. J. Craig, "Hybrid Position/Force Control of Manipulators", *ASME Journal of Dynamic Systems, Measurement and Control*, vol. 103, pp 126-133, 1981.

[12] R. G. Sanfelice, A. R. Teel, R. Goebel, C. Prieur "On the Robustness to Measurement Noise and Unmodeled Dynamics of Stability in Hybrid Systems", *Proc. 25th IEEE Amer. Cont. Conf.*, pp 4061-4066, 2006.

[13] T. Schlegl, M. Buss, G. Schmidt, "A Hybrid Systems Approach Toward Modeling and Dynamical Simulation of Dextrous Manipulation", *IEEE/ASME Trans. on Mechatronics*, vol. 8, n. 3, pp 352-361, 2003.

[14] M. Spong, "The Swing Up Control Problem for the Acrobot", *IEEE Control Systems Magazine*, vol. 15, n. 2, pp 49-55, 1995.

[15] T. Tarn, Y. Wu, N. Xi and A. Isidori, "Force Regulation and Contact Transition Control", *IEEE Cont. Sys. Mag.*, vol. 16, pp 32-40, 1996.